Work Summary

Done extensive tests on the choice of controls for double cavities. Simulated dynamics of [1,1] and performed variational method on [1,1] and [2,2].

Main Work

1. Derivation for hopping Hamiltonian of 3 electrons on 4 sites
2. Corrections and verification on half-filled Hubbard model's ground state energy
3. GRAPE parameter choice
4. Controls for double cavities model
5. Customized input pulses
6. Dynamics simulation
7. Variational method
8. Comments on a few potential directions

1 Derivation for hopping Hamiltonian of 3 electrons on 4 sites

For completeness, here gives the hopping Hamiltonian for 3 electrons on 4 sites, expressing in the basis of $\begin{pmatrix} |432\rangle \\ |431\rangle \\ |421\rangle \\ |321\rangle \end{pmatrix} = \begin{pmatrix} \hat{c}_4^\dagger \hat{c}_3^\dagger \hat{c}_2^\dagger |0\rangle \\ \hat{c}_4^\dagger \hat{c}_3^\dagger \hat{c}_1^\dagger |0\rangle \\ \hat{c}_4^\dagger \hat{c}_2^\dagger \hat{c}_1^\dagger |0\rangle \\ \hat{c}_3^\dagger \hat{c}_2^\dagger \hat{c}_1^\dagger |0\rangle \end{pmatrix}$.

The Hamiltonian elements are shown in Equation 1. Note that here t replaces the notation of J for clarity. This expression is the same as 1 electron hopping on 4 sites, and this can be understood as one hole hopping on 4 sites.

$$\hat{H}_{3e} = -t \begin{pmatrix} 0 & 1 & 0 & 1 \\ 1 & 0 & 1 & 0 \\ 0 & 1 & 0 & 1 \\ 1 & 0 & 1 & 0 \end{pmatrix} \tag{1}$$

2 Corrections and verification on half-filled Hubbard model's ground state energy

Previously I have calculated the ground state energy of the half-filled Hubbard model with 2 spin up 2 spin down on 4 sites. However, I made some mistakes on the plus-minus signs. Below is a corrected version.

$$
\begin{aligned}
\frac{\hat{T}_+}{-t}|\uparrow\uparrow\downarrow\downarrow\rangle &= -|-,\uparrow,\downarrow,\uparrow\downarrow\rangle + |\uparrow,-,\uparrow\downarrow,\downarrow\rangle - |\uparrow\downarrow,\uparrow,\downarrow,-\rangle + |\uparrow,\uparrow\downarrow,-,\downarrow\rangle \\
\frac{\hat{T}_+}{-t}|\downarrow\uparrow\uparrow\downarrow\rangle &= |-,\uparrow\downarrow,\uparrow,\downarrow\rangle + |\uparrow\downarrow,-,\uparrow,\downarrow\rangle + |\downarrow,\uparrow,-,\uparrow\downarrow\rangle + |\downarrow,\uparrow,\uparrow\downarrow,-\rangle \\
\frac{\hat{T}_+}{-t}|\downarrow\downarrow\uparrow\uparrow\rangle &= -|-,\downarrow,\uparrow,\uparrow\downarrow\rangle + |\downarrow,-,\uparrow\downarrow,\uparrow\rangle + |\downarrow,\uparrow\downarrow,-,\uparrow\rangle - |\uparrow\downarrow,\downarrow,\uparrow,-\rangle \\
\frac{\hat{T}_+}{-t}|\uparrow\downarrow\downarrow\uparrow\rangle &= |-,\uparrow\downarrow,\downarrow,\uparrow\rangle + |\uparrow\downarrow,-,\downarrow,\uparrow\rangle + |\uparrow,\downarrow,-,\uparrow\downarrow\rangle + |\uparrow,\downarrow,\uparrow\downarrow,-\rangle \\
\frac{\hat{T}_+}{-t}|\uparrow\downarrow\uparrow\downarrow\rangle &= |-,\uparrow\downarrow,\uparrow,\downarrow\rangle - |-,\downarrow,\uparrow,\uparrow\downarrow\rangle + |\uparrow\downarrow,-,\uparrow,\downarrow\rangle + |\uparrow,-,\uparrow\downarrow,\downarrow\rangle \\
&\quad + |\uparrow,\uparrow\downarrow,-,\downarrow\rangle + |\uparrow,\downarrow,-,\uparrow\downarrow\rangle + |\uparrow,\downarrow,\uparrow\downarrow,-\rangle - |\uparrow\downarrow,\downarrow,\uparrow,-\rangle \\
\frac{\hat{T}_+}{-t}|\downarrow\uparrow\downarrow\uparrow\rangle &= +|-,\uparrow\downarrow,\downarrow,\uparrow\rangle - |-,\uparrow,\downarrow,\uparrow\downarrow\rangle + |\uparrow\downarrow,-,\downarrow,\uparrow\rangle + |\downarrow,-,\uparrow\downarrow,\uparrow\rangle \\
&\quad + |\downarrow,\uparrow\downarrow,-,\uparrow\rangle + |\downarrow,\uparrow\ -,\uparrow\downarrow\rangle + |\downarrow,\uparrow,\uparrow\downarrow,-\rangle - |\uparrow\downarrow,\uparrow,\downarrow,-\rangle
\end{aligned} \tag{2}
$$

Expressing in the basis of $\begin{pmatrix} |\uparrow\uparrow\downarrow\downarrow\rangle \\ |\downarrow\uparrow\uparrow\downarrow\rangle \\ |\downarrow\downarrow\uparrow\uparrow\rangle \\ |\uparrow\downarrow\downarrow\uparrow\rangle \\ |\uparrow\downarrow\uparrow\downarrow\rangle \\ |\downarrow\uparrow\downarrow\uparrow\rangle \end{pmatrix}$, the effective Hamiltonian is then $-\frac{t^2}{U}\begin{pmatrix} 4 & 0 & 0 & 0 & 2 & 2 \\ 0 & 4 & 0 & 0 & 2 & 2 \\ 0 & 0 & 4 & 0 & 2 & 2 \\ 0 & 0 & 0 & 4 & 2 & 2 \\ 2 & 2 & 2 & 2 & 8 & 0 \\ 2 & 2 & 2 & 2 & 0 & 8 \end{pmatrix}$.
Finding the lowest eigenvalue of this matrix gives the ground state energy $E_{ground} = -12\frac{t^2}{U}$. The corresponding ground state is $\frac{1}{2\sqrt{3}}\begin{pmatrix} 1 \\ 1 \\ 1 \\ 1 \\ 2 \\ 2 \end{pmatrix}$. The energy of the *Néel* states are $\langle\downarrow\uparrow\downarrow\uparrow|\hat{H}'|\downarrow\uparrow\downarrow\uparrow\rangle = -\frac{4t^2}{U}$, which is $\frac{8t^2}{U}$ above the ground state.

As a verification, Figure 1 gives the plot of ground state energy in units of U vs the ratio of t/U. In the limit of small t/U, i.e. strongly correlated electrons, the ground state given by diagonalization fits well to the theoretically predicted ground state of $E_{ground} = -12\frac{t^2}{U}$. In the limit of high t/U, as derived before, the ground state energy should tend to -4t, i.e. linear.

Question: to verify the energy of the *Néel* states, then I'll need to apply the inverse of the unitary, i.e. the state should be $e^{-\frac{\hat{T}_+ - \hat{T}_-}{U}}|\downarrow\uparrow\downarrow\uparrow\rangle$. In this case, what values should $\hat{T}_+$ and $\hat{T}_-$ take?

3 GRAPE parameter choice

Following from previous results, it is crucial to choose appropriate parameters for the GRAPE algorithm to have reasonable run time while maintaining optimum performance. Two parameters of particular importance are the dimension of the truncated Hilbert space for the cavity and the number of time slices set for the piece-wise constant control. Just to give a sense of how large the parameters should be, some tests are done with single cavities first.

Since the spinless fermions can not occupy the same state, there is no nearest neighbor interaction involved, and only hopping is considered. Expressing as electrons, these spinless fermions are 'equiv-

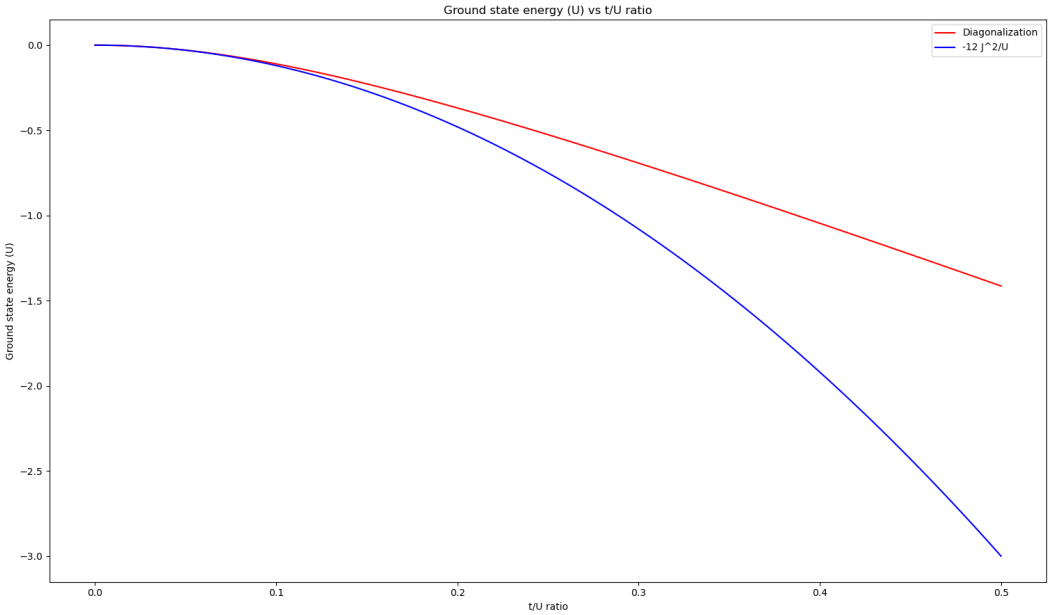

Figure 1: Ground state energy of half-filled Hubbard model with 4 sites

alent' to having all spin-up electrons since there is no flipping Hamiltonian considered that converts electrons of different spins. Thus, the results are of reference to cases when the hopping Hamiltonian is dominant compared to the nearest neighbor interaction. Note that as derived above, the hopping Hamiltonian for 3 spin-up electrons is the same as 1 spin-up electron, so the requirements on parameters should be the same.

Note that when finding the optimum value of N_{cav}, the absolute error is between the cost function, i.e. infidelity or energy, computed in the truncated Hilbert space compared to the cost function computed with the same control amplitudes in a large enough Hilbert space.

3.1 Dynamics simulation

With a single cavity, Figure 2 shows the infidelity vs the truncated Hilbert space dimension and infidelity vs number of time slices. It is observed that when dominated by hopping Hamiltonian, there should be $N_{cav} = 10$ and $N_{ts} = 40$ for cavities simulating 1 spin-up electron and $N_{cav} = 16$ and $N_{ts} = 60$ for cavities simulating 2 spin-up electrons.

3.2 Variational method

Similar plots are generated for variational method in Figure 3. Since the optimization objective is very different, the requirements do not need to be the same as dynamics simulation. It is observed that when dominated by hopping Hamiltonian, there should be $N_{cav} = 8$ and $N_{ts} = 40$ for cavities simulating 1 spin-up electron and $N_{cav} = 10$ and $N_{ts} = 60$ for cavities simulating 2 spin-up electrons.

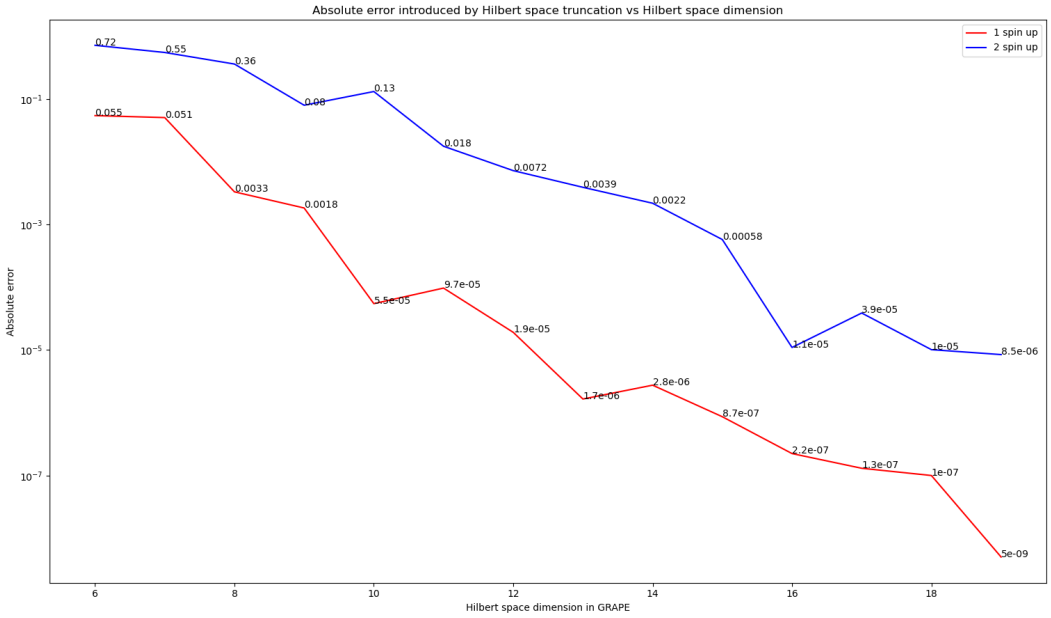

(a) Absolute error in infidelity vs dimension of truncated Hilbert space

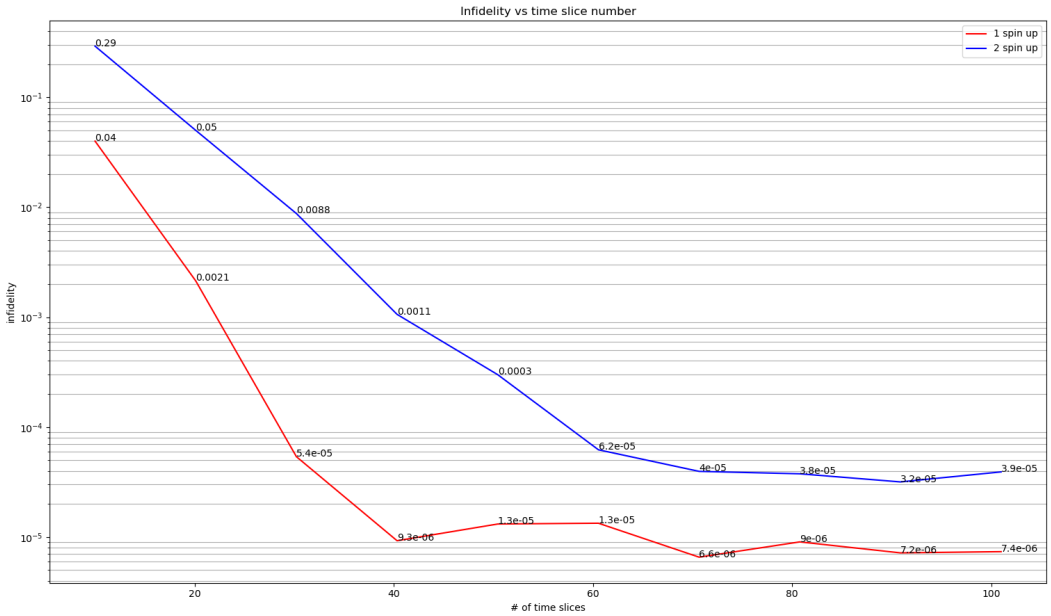

(b) Infidelity of dynamics simulation vs number of time slices.

Figure 2: Parameters choice for dynamics simulation. Results are shown for both 1 and 2 spin-up electrons.

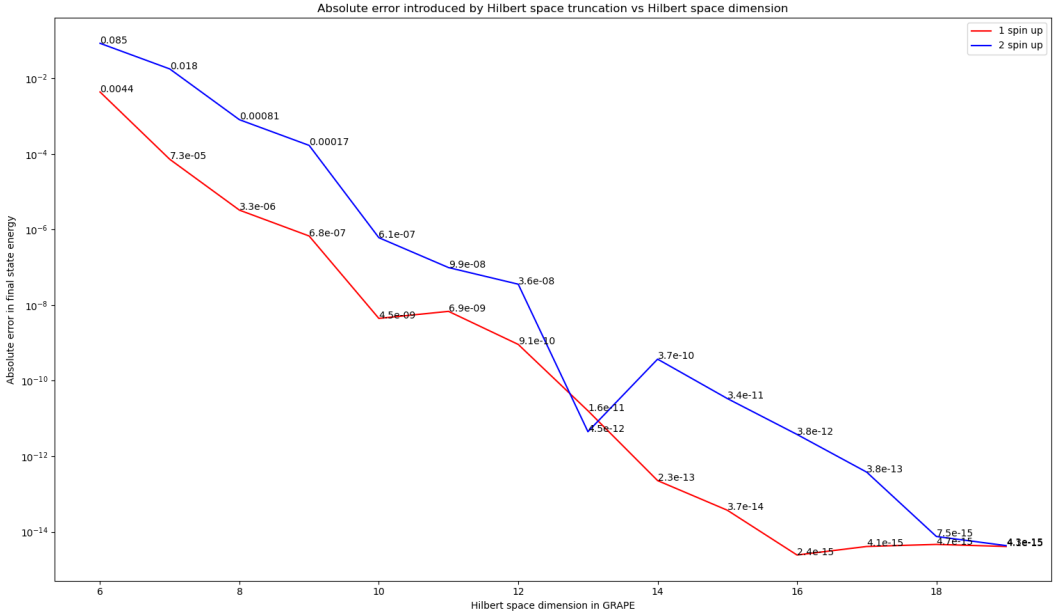

(a) Absolute error in final state energy vs dimension of truncated Hilbert space

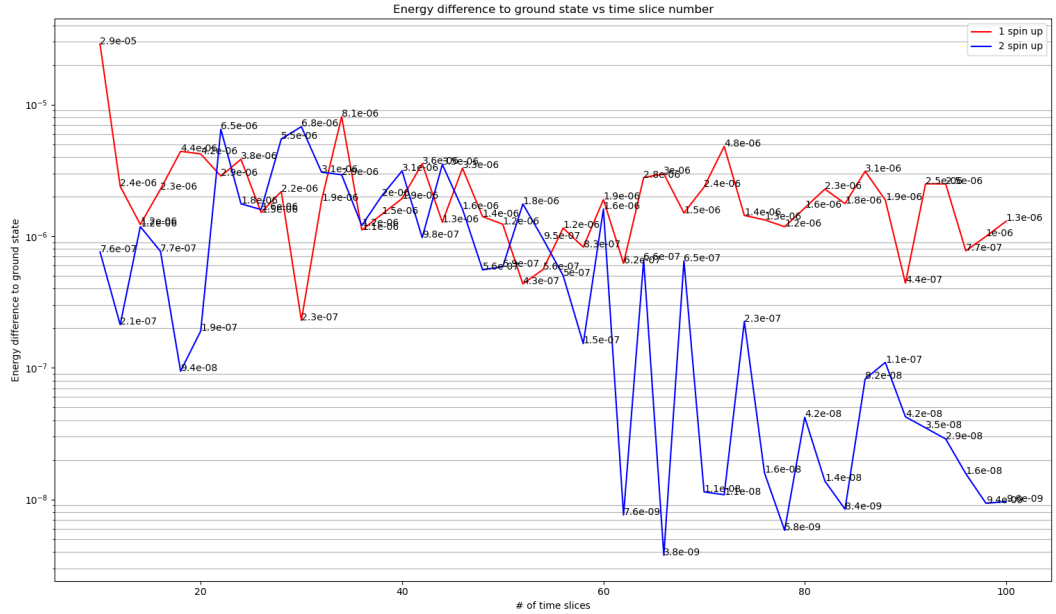

(b) Energy difference between final state and ground state vs number of time slices.

Figure 3: Parameters choice for dynamics simulation. Results are shown for both 1 and 2 spin-up electrons.

4 Controls for double cavities model

For double cavities, the controls needed to simulate dynamics are the controls on the individual cavities expressed as

$$\left\{\hat{a}_1 + \hat{a}_1^\dagger, i\left(\hat{a}_1 - \hat{a}_1^\dagger\right), \sigma_{1,x}, \sigma_{1,y}\right\} \text{ and } \left\{\hat{a}_2 + \hat{a}_2^\dagger, i\left(\hat{a}_2 - \hat{a}_2^\dagger\right), \sigma_{2,x}, \sigma_{2,y}\right\}.$$

In order to have the two cavities talk to each other, there is also the controls from the beam splitter that takes photon from one cavity to another

$$\left\{\hat{a}_1^\dagger \hat{a}_2 + \hat{a}_1 \hat{a}_2^\dagger, i\left(\hat{a}_1^\dagger \hat{a}_2 - \hat{a}_1 \hat{a}_2^\dagger\right)\right\}$$

and the controls from the mode squeezer

$$\left\{\hat{a}_1^\dagger \hat{a}_2^\dagger + \hat{a}_1 \hat{a}_2, i\left(\hat{a}_1^\dagger \hat{a}_2^\dagger - \hat{a}_1 \hat{a}_2\right)\right\}.$$

However, if symmetries are taken into account, simplifications can be made. Symmetries exist when the number of spin-up and spin-down electrons are the same, i.e. [1,1], [2,2], or [3,3]. In these cases, symmetry implies that if there is some control amplitude that simulates the dynamics, they should be identical on each cavity. Therefore the cavity controls can be reduced to

$$\left\{\hat{a}_1 + \hat{a}_1^\dagger + \hat{a}_2 + \hat{a}_2^\dagger, i\left(\hat{a}_2 - \hat{a}_2^\dagger\right) + i\left(\hat{a}_1 - \hat{a}_1^\dagger\right), \sigma_{1,x} + \sigma_{2,x}, \sigma_{1,y} + \sigma_{2,y}\right\}.$$

Similarly, the controls on the interactions between the cavities should have similar symmetries. For symmetric beam splitter control, it is modified to be

$$\left\{\hat{a}_1^\dagger \hat{a}_2 + \hat{a}_1 \hat{a}_2^\dagger\right\},$$

while it stays the same for the mode squeezer controls (Unfortunately I just realized this when writing this report. In the following, symmetric mode squeezer controls refers to only the first term of the control. I thought the second term is anti-symmetric like the beam splitter controls.).

The following table gives a reference of the 'nicknames' I gave the control types which appear in labels later on. The first two are the options for the cavity controls and the rest are for the interaction controls. For the ease of coding, an example of control label is "identical_symbs", which means using identical cavity controls and beam splitter controls with symmetry.

Controls		
Control terms	Names	Nicknames
$\left\{\hat{a}_1+\hat{a}_1^\dagger, i\left(\hat{a}_1-\hat{a}_1^\dagger\right), \sigma_{1,x}, \sigma_{1,y}\right\}$ and $\left\{\hat{a}_2+\hat{a}_2^\dagger, i\left(\hat{a}_2-\hat{a}_2^\dagger\right), \sigma_{2,x}, \sigma_{2,y}\right\}$	Independent controls	independent
$\left\{\hat{a}_1+\hat{a}_1^\dagger+\hat{a}_2+\hat{a}_2^\dagger, i\left(\hat{a}_2-\hat{a}_2^\dagger\right)+i\left(\hat{a}_1-\hat{a}_1^\dagger\right), \sigma_{1,x}+\sigma_{2,x}, \sigma_{1,y}+\sigma_{2,y}\right\}$	Identical controls	identical
No individual controls on the cavities		noCav
$\left\{\hat{a}_1^\dagger\hat{a}_2+\hat{a}_1\hat{a}_2^\dagger, i\left(\hat{a}_1^\dagger\hat{a}_2-\hat{a}_1\hat{a}_2^\dagger\right)\right\}$	Beam splitter	bs
$\left\{\hat{a}_1^\dagger\hat{a}_2+\hat{a}_1\hat{a}_2^\dagger\right\}$	Beam splitter with symmtry	symbs
$\left\{\hat{a}_1^\dagger\hat{a}_2^\dagger+\hat{a}_1\hat{a}_2, i\left(\hat{a}_1^\dagger\hat{a}_2^\dagger-\hat{a}_1\hat{a}_2\right)\right\}$	Mode squeezer	sq
$\left\{\hat{a}_1^\dagger\hat{a}_2^\dagger+\hat{a}_1\hat{a}_2\right\}$	Mode squeezer with symmtry	symsq
No interaction controls between cavities		noInt

5 Customized input pulses

One problem of the QuTip's built-in implementation of GRAPE is that it does not support customized input pulses. After modifying the source code again, I can now input customized pulses. This brings the following two possible directions.

5.1 Pre-optimization

Previously, the pulses acting on double cavities are set to random initially and then optimized. However, optimizing the pulses under double cavities can be computationally inefficient. One way to go is to optimize the pulse under singe cavity, and then input the pulse into the double cavities according to how many spin-up and spin-down electrons there are in each cavity. However, this is only suited for cases where the hopping Hamiltonian is dominant, i.e. $t \gg U$, so U can be treated as a perturbation. Examples will be shown in section 6.3.2.

5.2 Adiabatic method

Another way of treating t or U as perturbation is to turn on the dominant field first, then optimize the pulses. After a while, increase the perturbative field slightly and set the previously optimized pulse as the input pulse again into the algorithm. Repeat the previous process until the perturbative field is reaches the target magnitude. In this case, it can deal with either t or U as the perturbation. Examples will be shown in 6.3.3.

6 Dynamics simulation

6.1 Comparisons of models with standard parameters

First, define the standard parameters to be simulating [1,1] with double cavities. The Hamiltonian parameters have $\chi/t = 40$ and $t\tau \approx 1$, where τ is the pulse sequence duration. Note here that no site Hamiltonian are added. The number of time slices is 40. Figure 4 to 8 then shows plots of infidelity vs iterations for different controls types under different U/t ratios. A few remarks are as follows:

- The scaling of the x and y axis are deliberating set to be the same for each plot. It is pretty obvious that as U/t increases, the infidelity increases significantly.
  - The controls are having trouble simulating the tricky unitary U which only applies if the two cavities are at the same level.
  - As a result of the previous point, the capability of the controls to simulate U is much weaker than J. This is addressed in section 6.3.1.
- Among all control types, the ones with identical controls on the cavities perform better than the ones with independent controls. Although with small difference, controls of type "identical_symbs" seems to perform the best, but this is when I have given the incomplete expression of "symsq" as I described before.
- The restricting factor of the algorithm is commonly set to be the run time for these plots. It can be seen that as expected, the ones with less controls run more iterations than the ones with more controls.

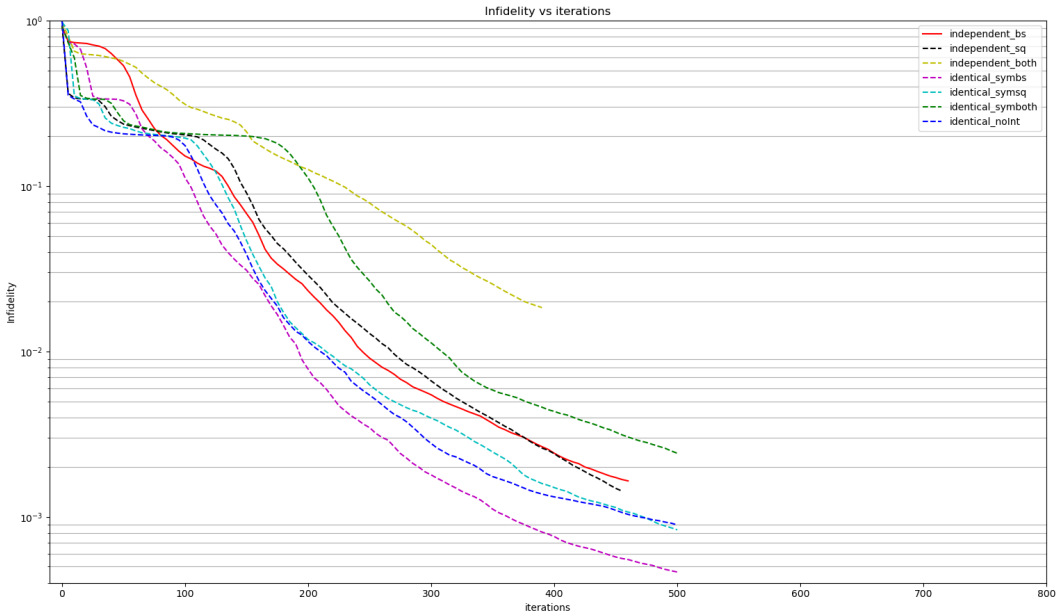

Figure 4: Performance of different control types under $U/t = 0.0$.

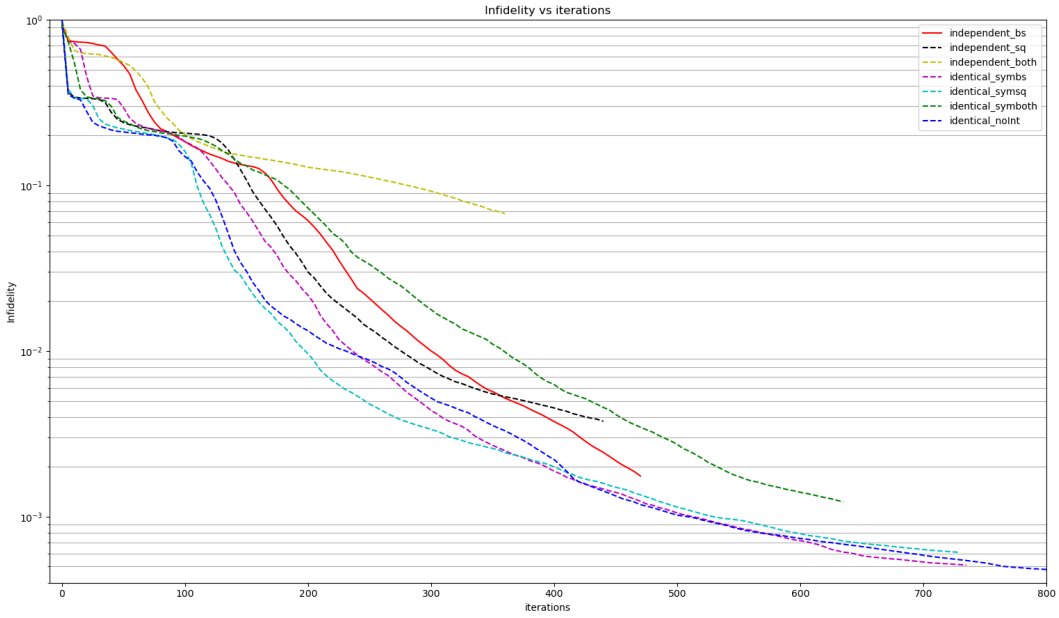

Figure 5: Performance of different control types under $U/t = 0.1$.

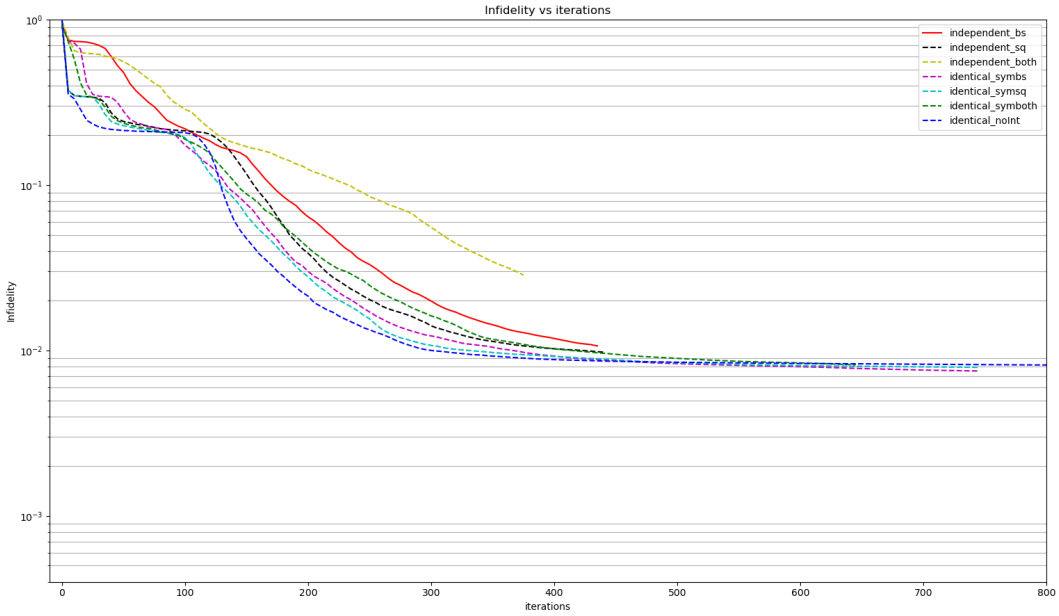

Figure 6: Performance of different control types under $U/t = 0.5$.

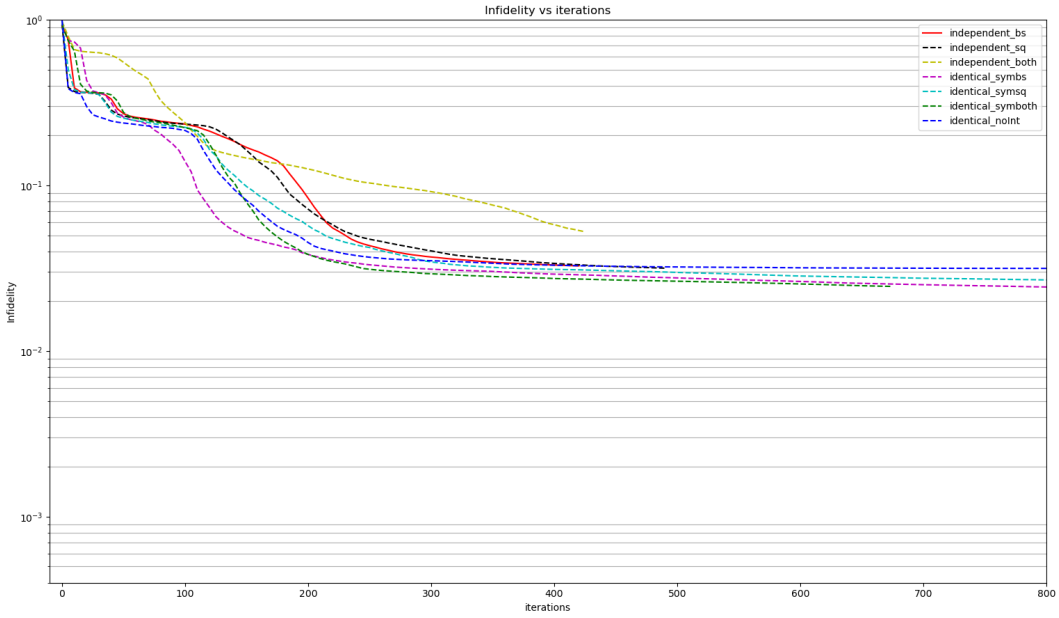

Figure 7: Performance of different control types under $U/t = 1.0$.

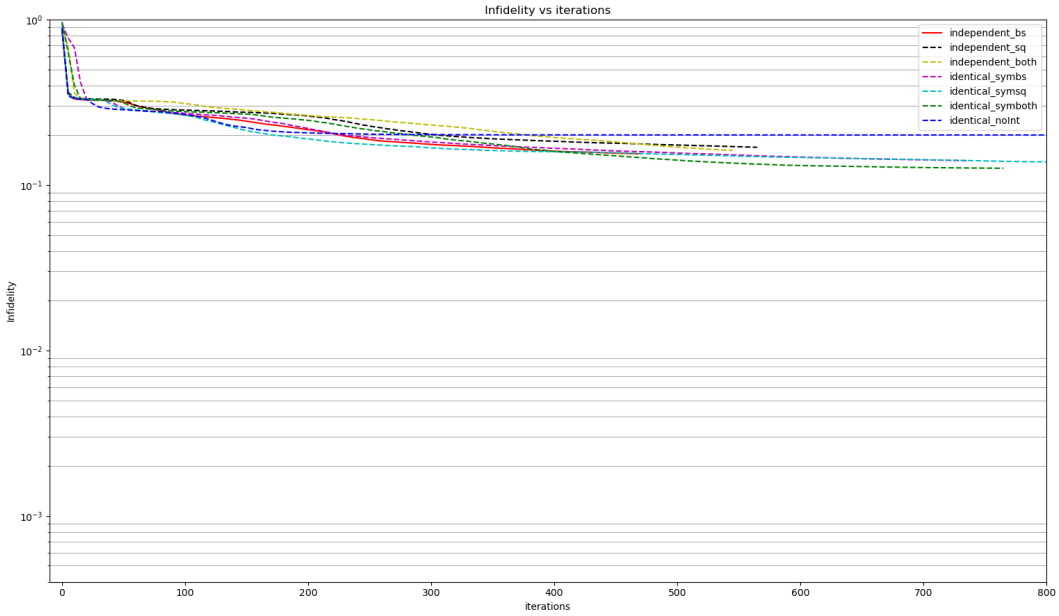

Figure 8: Performance of different control types under $U/t = 10.0$.

6.2 Pulse amplitude comparisons

The initial pulse shapes for controls are set to randomized piece-wise constant pulse of amplitude 1.0. While the optimized amplitude of the individual cavity controls all rise to around the scale of 10.0 or 20.0, the optimized amplitude of the interaction controls between cavities changes noticeably with U/t. Figure 9 shows the final optimized amplitude for control type "identical_symboth" when U/t = 0.1, 0.5, 1.0, and 10.0. To give a feeling of the magnitude, the drift Hamiltonian magnitude is $2\pi\chi$, where $\chi = 2.2$ in units of MHz.

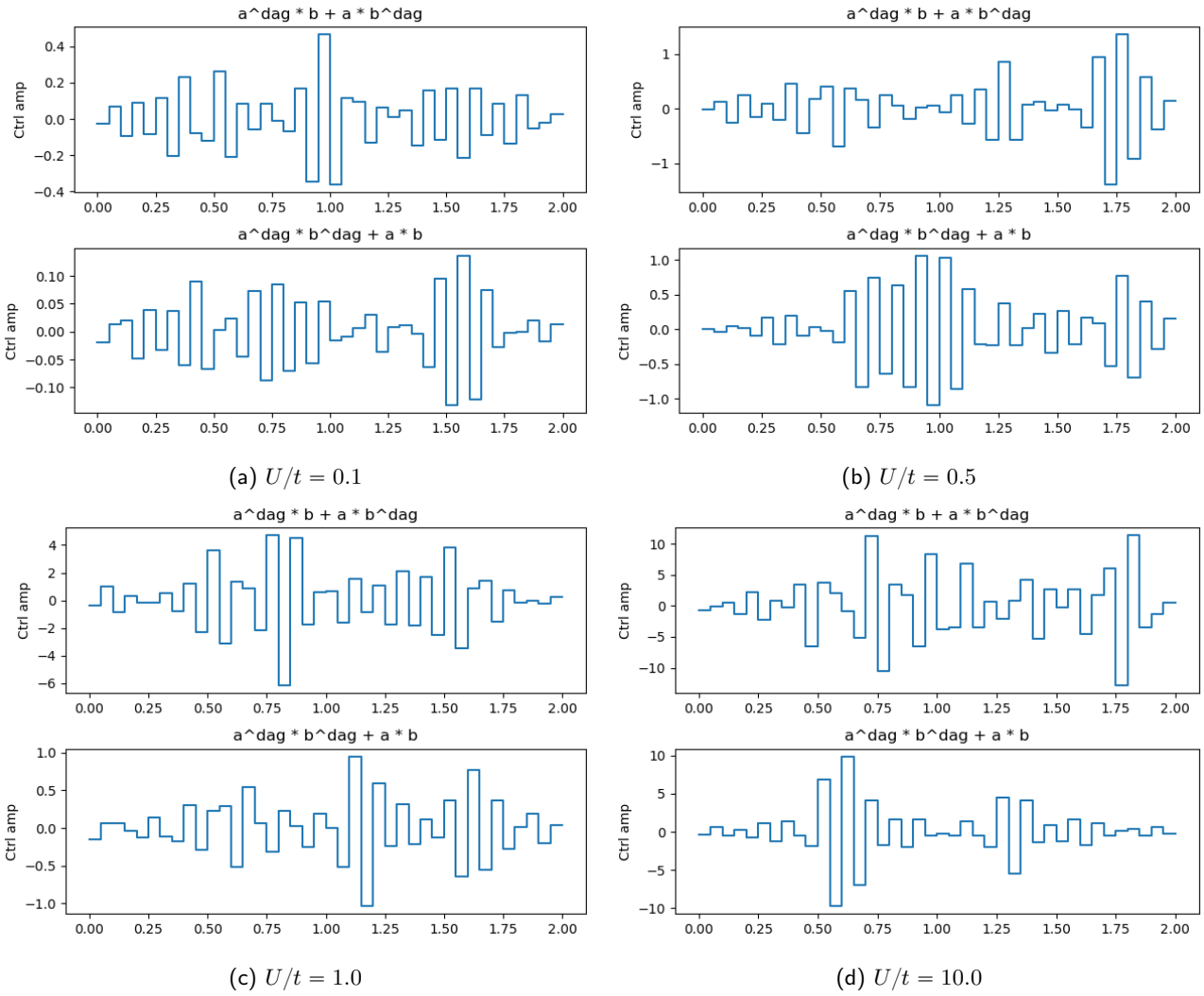

(a) $U/t = 0.1$

(b) $U/t = 0.5$

(c) $U/t = 1.0$

(d) $U/t = 10.0$

Figure 9: Optimized pulse amplitudes for the symmetric beam splitter and model squeezer controls under different ratio of U/t.

6.3 Special cases

6.3.1 No hopping, only nearest-neighbor interaction

In this case, t = 0 and U is measured through χ/U. This is essentially switching positions of U and t to see the capability of control when U and t are at the same magnitude. The results are shown in Figure 10.

It can be seen that indeed the infidelity at $\chi/U = 40$ is much lower than that at $\chi/t = 40$. Thus showing U is tricky to simulate. One other observation is that when the control type is "noCav_symboth", i.e. there is no control on individual cavities, the infidelity converges very fast to a local minimum.

A question: For single cavity, I remember it is said to have universal control given the 2 complex controls on the quadratures. In this case of t=0, it can be seen as attempting to use the symmetric beam splitter and mode squeezer controls to simulate solely the nearest-neighbor interactions, which in our encoding is essentially interactions between cavities. Is the combination of symmetric beam splitter and mode squeezer controls enough for universal control between cavities? The results in Figure 10 seems to not imply so.

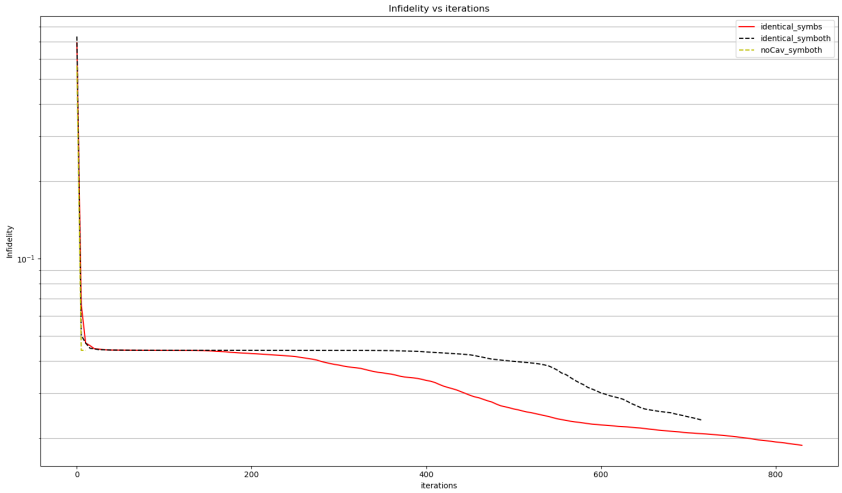

(a) $\chi/U = 40$

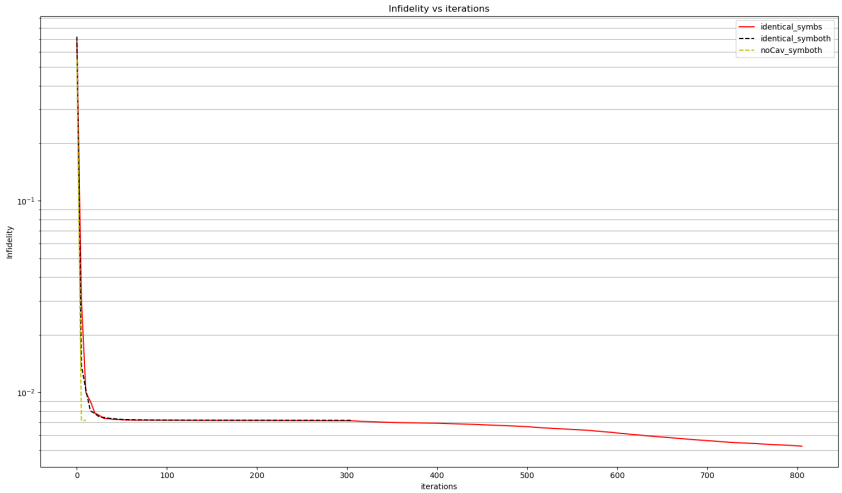

(b) $\chi/U = 100$

Figure 10: Performance of different control types when t = 0 and under different χ/U.

6.3.2 Pre-optimized pulse

Simulate dynamics of 1 electron in single cavity first. The resulting infidelity is around 10^{-5}. Then input the optimized pulse symmetrically to the individual cavities, and set the controls of cavity interaction to be symmetric beam splitter and mode squeezer, i.e. symboth, and their initial amplitudes to be zero. Let the physical model have the standard parameters with $U/t = 0.5$. The results are shown in Figure 11. While the infidelity is already pretty low in the beginning as expected, the decrease in the infidelity is relatively slow.

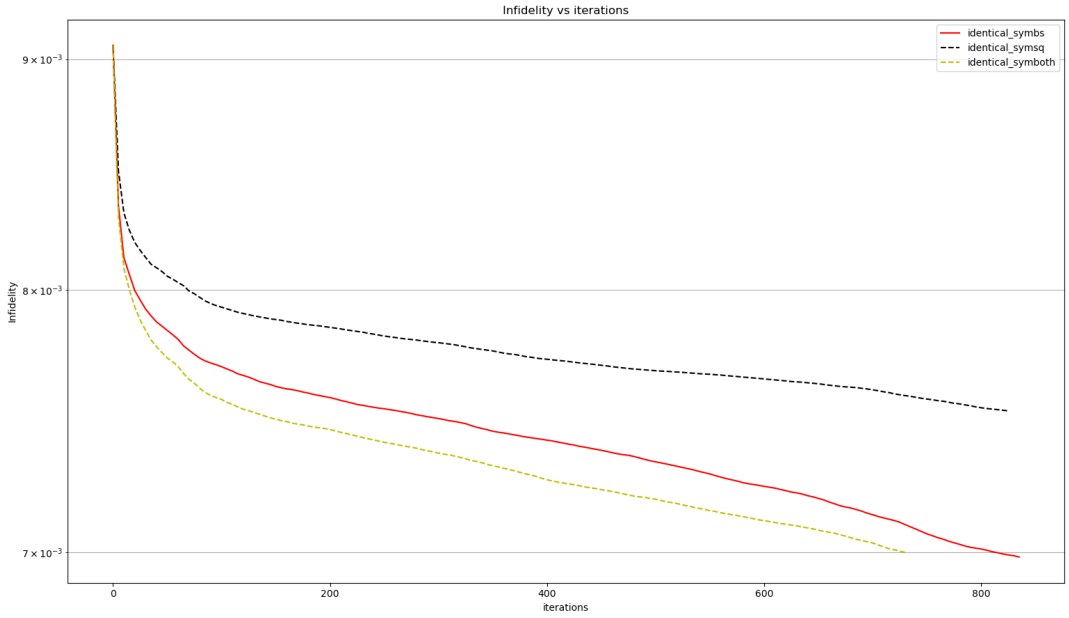

Figure 11: Performance of different control types under $U/t = 0.5$ with pre-optimized pulses.

6.3.3 Adiabatic method

Just as an illustration of the working adiabatic method, an example is shown in Figure **??**, where it is optimized for standard parameters and $U/t = 0.5$. Note that similarly pre-optimized pulses are used as inputs. As expected, for the adiabatic method, the infidelity decreases during each round of GRAPE, but then increases when more of U is rised higher. Thus, the resulting shape is the step-like curve shown. I have experimented with the adiabatic method in different parameters settings, but it hasn't shown significant advantages yet, mostly performing at the same level as the normal method.

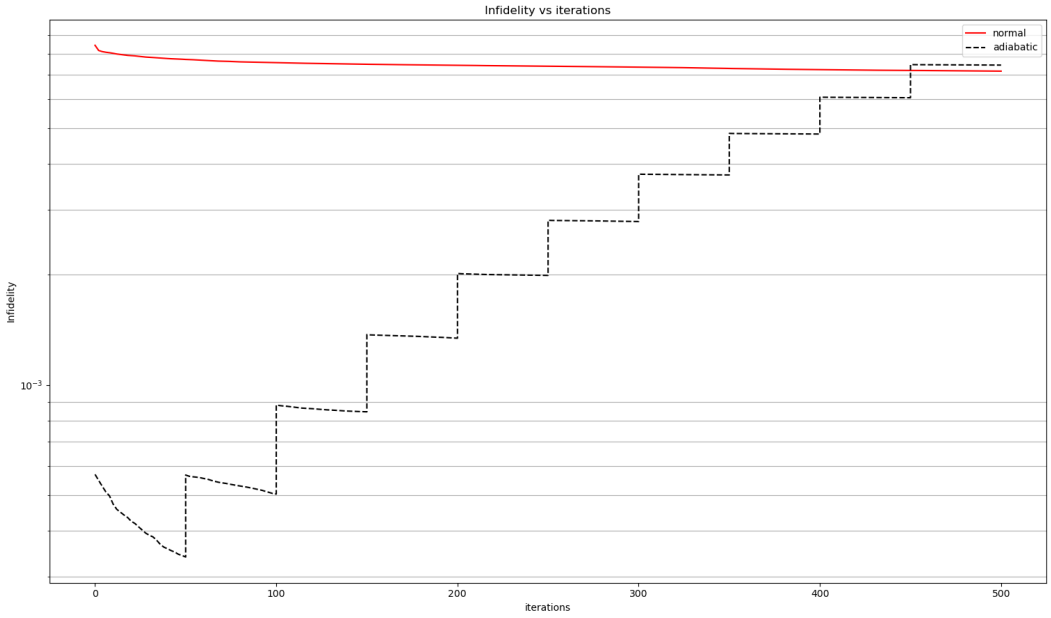

Figure 12: Performance of adiabatic method and normal method, i.e. adding U in the beginning, under $U/t = 0.5$ with pre-optimized pulses.

7 Variational method

For dynamics, as shown in the section of choosing the parameters, the required N_{cav} to run [2,2] accurately is around 16 levels, which is prohibitive for the current computing resources I have. Thus, all previous results from dynamics simulations are done on [1,1]. For variational method, only 10 levels are required when hopping is dominant, thus allowing some results for [2,2].

7.1 1 spin up, 1 spin down

Results are shown from Figure 13 to 15. In general the infidelity increases as U/t increases as expected. However, I thought that having control type "identical_noInt" should be good enough because the ground state does not really require simulating the inter-cavity Hamiltonian. It is just about reaching a target state that minizes the expected energy. In this case, having universal control on independent cavities should be enough. (Is this true?)

However, the results in Figure 14 and 15 seems to imply that having "identical_noInt" can easily get stuck in local minima. Might not be obvious from the plots, but in Figure 15, the energy that

"identical_noInt" converges to is state of E=0, which is an eigenstate of the Hamiltonian and is very close to the actual ground state when nearest-neighbor interaction dominates.

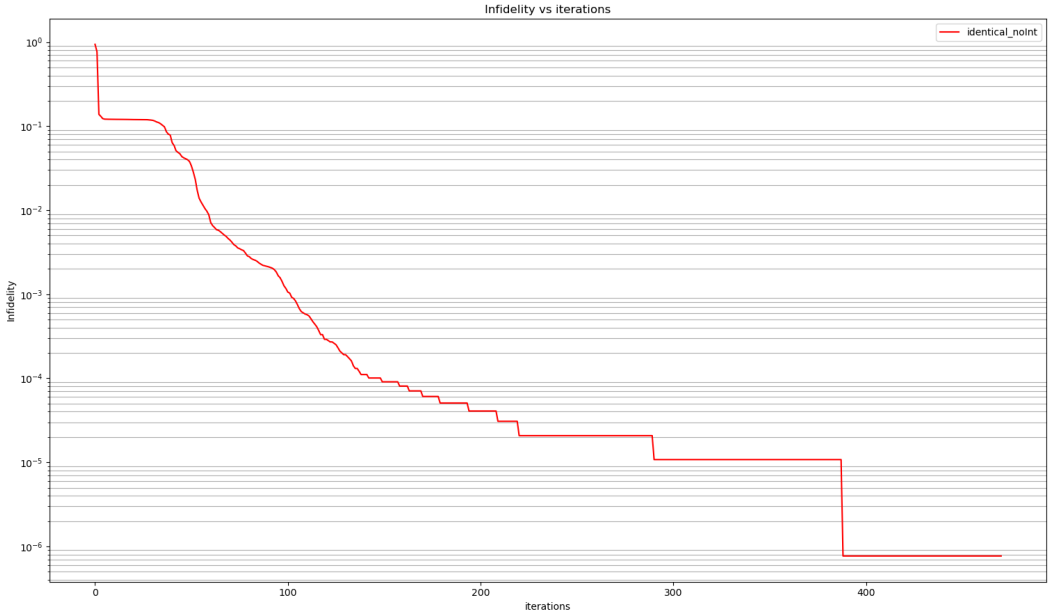

Figure 13: Energy difference to ground state at $\chi/t = 40$ and $U/t = 0.0$.

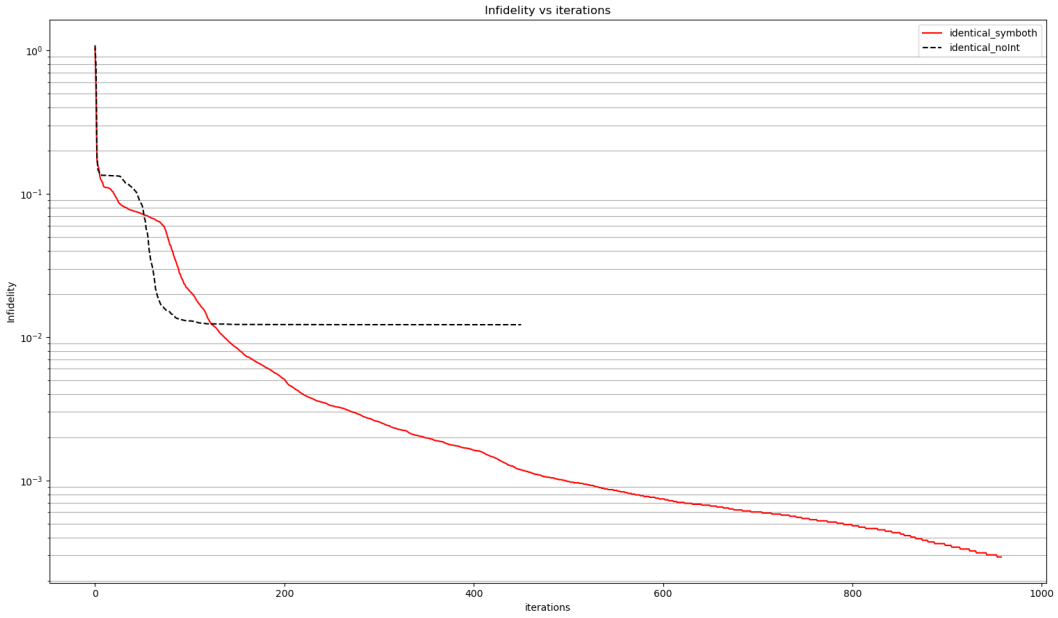

Figure 14: Energy difference to ground state at $\chi/t = 40$ and $U/t = 1.0$.

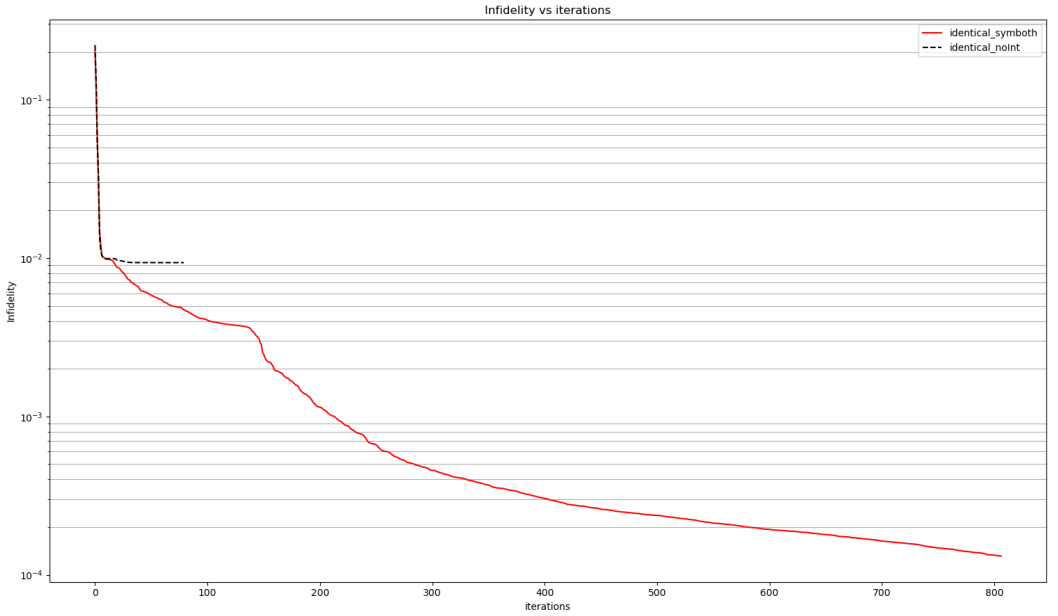

Figure 15: Energy difference to ground state at $\chi/t = 4000$ and $U/t = 100.0$.

7.2 2 spin up, 2 spin down

Similarly, the result for $U/t = 0.0$ is shown in Figure 16. The result for $\chi/t = 4000$ and $U/t = 100.0$ is not included here, but it looks very similar to the one in the previous section, i.e. the control type "identical_noInt" tends to get stuck in E=0 state.

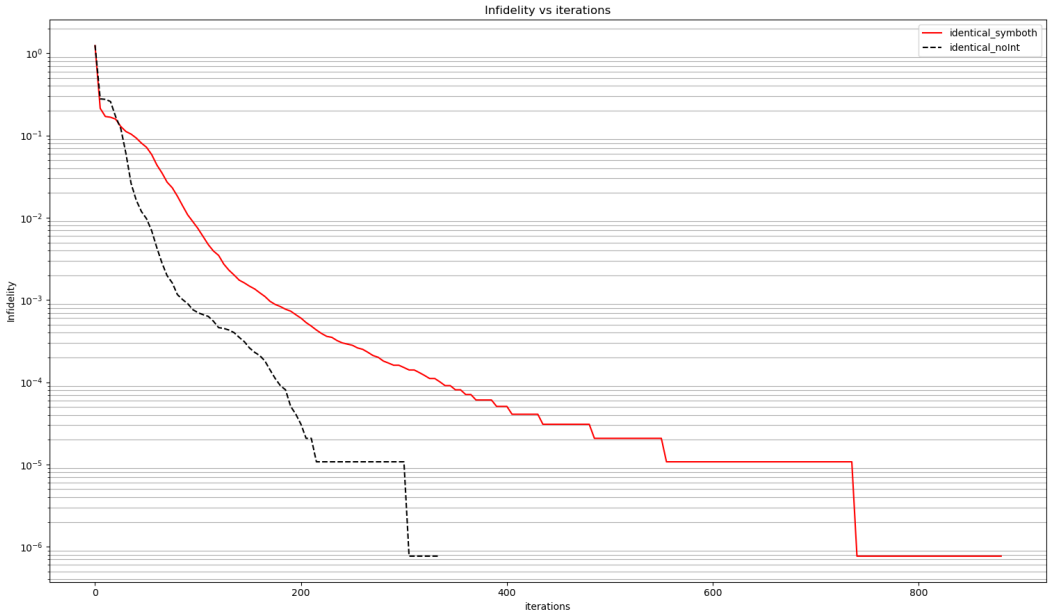

Figure 16: Energy difference to ground state at $\chi/t = 40$ and $U/t = 0.0$.

8 Comments on a few potential directions

8.1 Automatic differentiation

Automatic differentiation is a concept from the machine learning community. It defines a set of functions and corresponding derivatives, and computes the gradients using the computational graph models generated. This has already been combined with quantum optimal control algorithms such as GRAPE in open systems [1]. One of the main reasons they implemented auto-diff is that they have a open-system problem, which can't easily back-propagate the operators since they are not unitary. Their implementation is based on modules in Tensorflow, which supports multiprocessing and GPU computing. These properties starts to bring advantages for large Hilbert space dimensions over around 100 [2].

Conclusion: For the current stage, auto-diff is not really necessary since the analytic expression for the gradients with respect to the controls are clear under closed systems. However, if decoherence terms are included in the future, auto-diff can be advantageous.

8.2 Hamiltonian mapping from fermion basis to boson basis

As described before, special caution needs to be taken when mapping from fermion basis to boson basis. For example, in the two electron case, the first 6 cavity energy levels corresponds to electrons occupying sites $\begin{pmatrix} |21\rangle \\ |41\rangle \\ |31\rangle \\ |42\rangle \\ |32\rangle \\ |43\rangle \end{pmatrix}$. The mapping from the cavity level basis to the site basis can not be simply expressed in matrix as

$$\hat{A} = \begin{pmatrix} 1 & 1 & 1 & 0 & 0 & 0 \\ 1 & 0 & 0 & 1 & 1 & 0 \\ 0 & 0 & 1 & 0 & 1 & 1 \\ 0 & 1 & 0 & 1 & 0 & 1 \end{pmatrix}.$$

This can be shown since in cavity levels basis $\langle 31|41\rangle = 0$, but under this mapping, in sites basis $\langle 31|41\rangle = \left(\langle 3| + \langle 1|\right)\left(|4\rangle + |1\rangle\right) = 1$. Therefore, the appropriate way to go is for a general encoding $\begin{pmatrix} \hat{c}^\dagger_{i,\uparrow} \cdots \hat{c}^\dagger_{j,\downarrow}|0\rangle \\ \vdots \end{pmatrix}$ and a Hamiltonian in the site basis $\hat{H}\left(\hat{c}^\dagger_{i,\sigma}, \cdots\right)$, compute the corresponding matrix elements explicitly following the algebra. Example of Hamiltonians can be the nearest neighbor interaction

$$\hat{H}_{NN} = U \sum_i \hat{n}_{i,\uparrow} \otimes \hat{n}_{i,\downarrow},$$

in which case the encoding needs to be a tensor product of the up and down spins encoding. Some useful packages include openFermion and SymPy.

8.3 Krotov's algorithm

Krotov's algorithm is another optimal control algorithm. It is different with GRAPE in that it updates the control sequentially while GRAPE does that concurrently. The original implementation of GRAPE also don't guarantee monotonic convergence, while Krotov does. However, in the current version of

GRAPE, L-BFGS-B quasi-Newton method is used for optimization, which is second order. In this case, GRAPE normally converges monotonically as well. Lastly, Krotov produces smooth piece-wise constant control amplitudes, while GRAPE doesn't.

Conclusion: Krotov's algorithm can be a alternative to GRAPE, but I haven't found any theory suggesting that Krotov's algorithm is more suited for our specific problem.

References

[1] D. Schuster M. Abdelhafez and J. Koch. *Phys. Rev. A*, 99, 052327, 2019.

[2] J. Koch N. Leung, M. Abdelhafez and D. Schuster. *Phys. Rev. A*, 95, 042318, 2017.